

# The power continuous Bernoulli distribution: Theory and applications

CHRISTOPHE CHESNEAU<sup>1</sup>

FESTUS C. OPONE<sup>2</sup>



<sup>1</sup> Department of Mathematics, LMNO, University of Caen, 14032 Caen, France.

<sup>2</sup> Department of Statistics, University of Benin, Benin City, Nigeria.

christophe.chesneau@unicaen.fr<sup>1</sup>

festus.opone@physci.uniben.edu<sup>2</sup>

## Abstract

*The continuous Bernoulli distribution is a recently introduced one-parameter distribution with support  $[0, 1]$ , finding numerous applications in applied statistics. The idea of this article is to propose a natural extension of this distribution by adding a shape parameter through a power transformation. We introduce the power continuous Bernoulli distribution, aiming to extend the modeling scope of the continuous Bernoulli distribution. Basics of its mathematical properties are derived, such as the shapes of the related functions, the determination of various moment measures, and an evaluation of the overall amount of its randomness via the Rényi entropy. A statistical analysis of the distribution is then performed, showing how it can be applied when dealing with data. Estimates of the parameters are discussed through the maximum likelihood method. A Monte Carlo simulation study investigates the asymptotic behavior of these estimates. The flexibility of the power continuous Bernoulli distribution in real-life data fitting is analyzed using two data sets. Also, fair competitors are considered to highlight the accuracy of this distribution. At all stages, numerous graphics and tables illustrate the findings.*

**Keywords:** Continuous Bernoulli distribution; moments; quantiles; entropy; data fitting.

## 1. INTRODUCTION

In order to understand the mathematical foundation of the study, let us first present the so-called continuous Bernoulli distribution as introduced in [19].

**Definition 1.** The continuous Bernoulli distribution with parameter  $\lambda \in [0, 1]$ , also denoted as  $\mathcal{CB}(\lambda)$ , is defined by the following probability density function (pdf):

$$f(x; \lambda) = \begin{cases} 1, & \lambda = \frac{1}{2} \text{ and } x \in [0, 1], \\ c_\lambda \lambda^x (1 - \lambda)^{1-x}, & \lambda \in (0, 1) / \left\{ \frac{1}{2} \right\} \text{ and } x \in [0, 1], \\ 0, & x \notin [0, 1], \end{cases} \quad (1)$$

where  $c_\lambda$  is the following constant:

$$c_\lambda = \frac{2 \operatorname{arctanh}(1 - 2\lambda)}{1 - 2\lambda}. \quad (2)$$

Here,  $\operatorname{arctanh}(x)$  denotes the inverse hyperbolic tangent defined by  $\operatorname{arctanh}(x) = (1/2) \ln[(1 + x)/(1 - x)]$  (as a minor remark, the following expressions are equivalent:  $2 \operatorname{arctanh}(1 - 2\lambda) = \ln(1 - \lambda) - \ln(\lambda) = \ln(1/\lambda - 1)$ ).

Alternatively, the  $\mathcal{CB}(\lambda)$  distribution can be defined by its cumulative distribution function (cdf), which is given by

$$F(x; \lambda) = \begin{cases} 0, & x < 0, \\ x, & \lambda = \frac{1}{2} \text{ and } x \in [0, 1], \\ \frac{\lambda^x(1-\lambda)^{1-x} + \lambda - 1}{2\lambda - 1}, & \lambda \in (0, 1) / \left\{ \frac{1}{2} \right\} \text{ and } x \in [0, 1], \\ 1, & x > 1. \end{cases} \quad (3)$$

Thus, the  $\mathcal{CB}(\lambda)$  distribution, like the power distribution, is a one-parameter continuous distribution with support of  $[0, 1]$ . It is useful in a variety of fields, including probability theory, statistics, with an emphasis on machine learning. In particular, it is good at simulating the pixel intensities of natural images in deep learning and computer vision, especially when putting up variational autoencoders. We advise the reader to [19] and [13] for more information on these topics.

More broadly, bounded support distributions have proven useful in modeling real-world data, particularly in scenarios where the data are measured in percentages and proportions. So when the observations take on value within the unit interval  $[0, 1]$ . In recent decades, the beta and Kumaraswamy distributions have gained more popularity in this regard. However, there are situations where these classical distributions provide poor fit in data analysis. This has become a quest for many researchers to develop alternative bounded distributions with better flexibility in real-life data fitting. With this in mind, [12] introduced the log-Lindley distribution, [21] developed the unit-logistic distribution, [1] created the log-Xgamma distribution, [20] proposed the unit-Gompertz distribution, [23] developed the Kumaraswamy unit-Gompertz distribution, [16] examined the unit-Burr XII distribution, [15] introduced the unit-Chen distribution, [26] developed the transmuted Marshall-Olkin extended Topp-Leone distribution, [6] proposed the log-XLindley distribution, [2] studied the unit-Rayleigh distribution, etc. The  $\mathcal{CB}(\lambda)$  distribution belongs to the list.

In this paper, by including a shape parameter, we hope to increase the flexibility of the  $\mathcal{CB}(\lambda)$  distribution for a variety of applications. In other words, for a random variable  $X$  following the  $\mathcal{CB}(\lambda)$  distribution, we consider the distribution of the power random variable  $Y = X^{1/\alpha}$ , where  $\alpha > 0$ . In this way, we introduce the power continuous Bernoulli distribution with parameters  $\alpha$  and  $\lambda$ ,  $\mathcal{PCB}(\alpha, \lambda)$  distribution for short. The used power scheme is somewhat classic in statistics, and allows to flexibilize various "rigid distributions". We may mention the Weibull distribution, which is the power version of the exponential distribution, the power Lindley distribution by [9], which is the power version of the Lindley distribution (see [18]), etc. Recent examples include the power beta distribution by [5], the power Lomax distribution by [28], the power Ailamujia distribution by [14], etc.

In fact, at the time of writing, no extensions of the  $\mathcal{CB}(\lambda)$  distribution exist, and the  $\mathcal{PCB}(\alpha, \lambda)$  distribution is a strong contender for being useful from both theoretical and applied perspectives. After a detailed presentation, we investigate its main features, such as the related probability functions, moments of various kinds, and entropy (Rényi entropy). Then, we examine the practice on the statistical side. We estimate the  $\mathcal{PCB}(\alpha, \lambda)$  distribution parameters, i.e.,  $\alpha$  and  $\lambda$ , by the maximum likelihood (ML) method. A Monte Carlo simulation study is then conducted to validate the asymptotic behavior of these estimates. We present significant applications of the  $\mathcal{PCB}(\alpha, \lambda)$  distribution in a data fitting context, with the use of two real-life data sets: one containing trade share data, and the other containing tensile strength of polyester fibers. In addition, several distributions are considered for fair comparison in terms of efficiency in fitting. Illustrations, via tables and graphics, are given to support the findings. We have thus laid the foundation for the use of the  $\mathcal{PCB}(\alpha, \lambda)$  distribution for statistical purposes.

The organization of the paper is as follows: Section 2 describes the  $\mathcal{PCB}(\alpha, \lambda)$  distribution, including its underlying functions of interest. A moment analysis is performed in Section 3. The entropy is studied in Section 4. Parameter estimation, simulation study and real-life data fitting

are developed in Section 5. A conclusion is given in Section 6.

## 2. POWER CONTINUOUS BERNOULLI DISTRIBUTION

The  $\mathcal{PCB}(\alpha, \lambda)$  distribution is defined below through its related probabilistic functions.

**Definition 2.** Based on its stochastic definition and the functions (1) and (3), the  $\mathcal{PCB}(\alpha, \lambda)$  distribution with  $\alpha > 0$  and  $\lambda \in [0, 1]$  is defined by the following cdf:

$$F(x; \alpha, \lambda) = F(x^\alpha; \lambda) = \begin{cases} 0, & x < 0 \\ x^\alpha, & \lambda = \frac{1}{2} \text{ and } x \in [0, 1], \\ \frac{\lambda^{x^\alpha} (1 - \lambda)^{1 - x^\alpha} + \lambda - 1}{2\lambda - 1}, & \lambda \in (0, 1) / \left\{ \frac{1}{2} \right\} \text{ and } x \in [0, 1], \\ 1, & x > 1, \end{cases} \quad (4)$$

or, equivalently, by the following pdf:

$$f(x; \alpha, \lambda) = \alpha x^{\alpha-1} f(x^\alpha; \lambda) = \begin{cases} \alpha x^{\alpha-1}, & \lambda = \frac{1}{2} \text{ and } x \in [0, 1], \\ c_\lambda \alpha x^{\alpha-1} \lambda^{x^\alpha} (1 - \lambda)^{1 - x^\alpha}, & \lambda \in (0, 1) / \left\{ \frac{1}{2} \right\} \text{ and } x \in [0, 1], \\ 0, & x \notin [0, 1], \end{cases} \quad (5)$$

where  $c_\lambda$  is the constant defined in (2).

Basically, by taking  $\alpha = 1$  into (4) and (5), we obtain the cdf and pdf of the  $\mathcal{CB}(\lambda)$  distribution, as described in (3) and (1), respectively.

It is important to note that the  $\mathcal{PCB}(\alpha, \lambda)$  distribution has one mode in the case  $\lambda \in (1/2, 1)$ , and it is given by the following mathematical formula:  $x = [(\alpha - 1) / (2\alpha \operatorname{arctanh}(1 - 2\lambda))]^{1/\alpha}$ . In this case, the  $\mathcal{PCB}(\alpha, \lambda)$  distribution is unimodal, and the mode differs from 0 if, and only if,  $\alpha \in [0, 1)$ , i.e.,  $\alpha \neq 1$ . So by considering the power version of the  $\mathcal{CB}(\lambda)$  distribution, we introduce a unimodality property that can be used quite efficiently for statistical aims, including data fitting purposes.

Figure 1 presents the plots for  $f(x; \alpha, \lambda)$  in order to illustrate the effect of the parameter  $\alpha$  on its possible shapes.

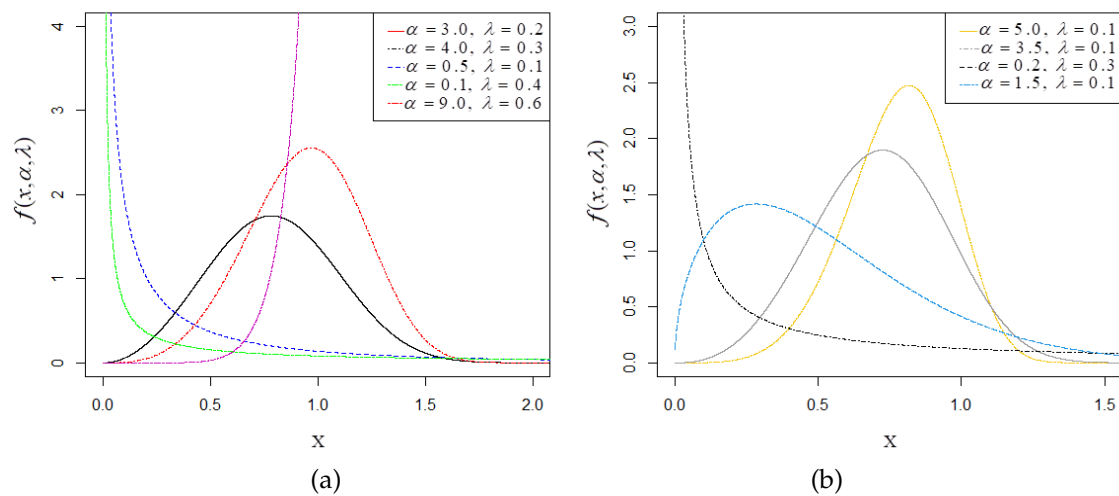


**Figure 1:** Pdf plots of the  $\mathcal{PCB}(\alpha, \lambda)$  distribution at different choices of the parameter settings: (a)  $(\alpha, \lambda) \in \{(3, 0.2), (4, 0.3), (0.5, 0.1), (0.1, 0.4), (9, 0.6)\}$  and (b)  $(\alpha, \lambda) \in \{(5, 0.1), (3.5, 0.1), (0.2, 0.3), (1.5, 0.1)\}$

Clearly, we observe that the pdf of the  $\mathcal{PCB}(\alpha, \lambda)$  distribution accommodates decreasing (reversed-J) or increasing, left-skewed, right-skewed and symmetric shapes.

As a complementary function to the pdf, the hazard rate function (hrf) of the  $\mathcal{PCB}(\alpha, \lambda)$  distribution is given as

$$h(x; \alpha, \lambda) = \frac{f(x; \alpha, \lambda)}{1 - F(x; \alpha, \lambda)} = \begin{cases} \frac{\alpha x^{\alpha-1}}{1 - x^\alpha}, & \lambda = \frac{1}{2} \text{ and } x \in [0, 1], \\ \frac{c_\lambda^* \alpha x^{\alpha-1} \lambda^{x^\alpha} (1 - \lambda)^{1-x^\alpha}}{\lambda - \lambda^{x^\alpha} (1 - \lambda)^{1-x^\alpha}}, & \lambda \in (0, 1) / \left\{ \frac{1}{2} \right\} \text{ and } x \in [0, 1], \\ 0, & x \notin [0, 1], \end{cases}$$

where  $c_\lambda^* = (2\lambda - 1)c_\lambda = -2 \operatorname{arctanh}(1 - 2\lambda)$ . The graphical representation of this function is displayed in Figure 2.

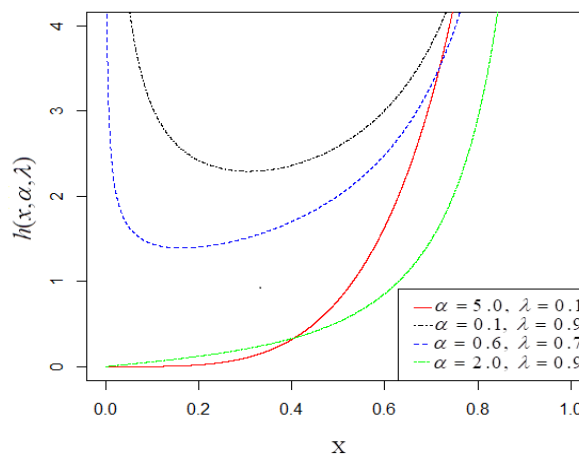


**Figure 2:** Hrf plots of the  $\mathcal{PCB}(\alpha, \lambda)$  distribution at different choices of the parameter settings:  $(\alpha, \lambda) \in \{(5, 0.1), (0.1, 0.9), (0.6, 0.7), (2, 0.9)\}$

Figure 2 indicates that the  $\mathcal{PCB}(\alpha, \lambda)$  distribution exhibits increasing and bathtub-shaped hazard properties. These are demanded properties for data analysis purposes with values in  $[0, 1]$ .

As the inverse function of the cdf, the quantile function (qf) of the  $\mathcal{PCB}(\alpha, \lambda)$  distribution is given as

$$Q(x; \alpha, \lambda) = F^{-1}(x; \alpha, \lambda) = \begin{cases} x^{1/\alpha}, & \lambda = \frac{1}{2} \text{ and } x \in [0, 1], \\ \left\{ \frac{\ln[(2\lambda - 1)x + 1 - \lambda] - \ln(1 - \lambda)}{\ln(\lambda) - \ln(1 - \lambda)} \right\}^{1/\alpha}, & \lambda \in (0, 1) / \left\{ \frac{1}{2} \right\} \text{ and } x \in [0, 1]. \end{cases} \quad (6)$$

By inserting  $x = 1/2$  in (6), we obtain the median of the  $\mathcal{PCB}(\alpha, \lambda)$  distribution, which is given by

$$M = \begin{cases} 2^{-1/\alpha}, & \lambda = \frac{1}{2}, \\ \left\{ \frac{\ln(2) + \ln(1 - \lambda)}{2 \operatorname{arctanh}(1 - 2\lambda)} \right\}^{1/\alpha}, & \lambda \in (0, 1) / \left\{ \frac{1}{2} \right\}. \end{cases}$$

Traditionally, the qf and random values from the uniform distribution over  $[0, 1]$  can be used to generate random values from a random variable  $Y$  following the  $\mathcal{PCB}(\alpha, \lambda)$  distribution. Table 1

shows some quantiles from the  $\mathcal{PCB}(\alpha, \lambda)$  distribution using the expression in (6) as illustrative numerical examples.

**Table 1:** Some values of the qf of the  $\mathcal{PCB}(\alpha, \lambda)$  distribution.

| $x$  | $\alpha = 0.5, \lambda = 0.3$ | $\alpha = 0.5, \lambda = 0.8$ | $\alpha = 1, \lambda = 0.3$ | $\alpha = 1, \lambda = 0.8$ |
|------|-------------------------------|-------------------------------|-----------------------------|-----------------------------|
| 0.05 | 0.0012                        | 0.0102                        | 0.0342                      | 0.1008                      |
| 0.1  | 0.0048                        | 0.0358                        | 0.0694                      | 0.1893                      |
| 0.2  | 0.0205                        | 0.1149                        | 0.1432                      | 0.3390                      |
| 0.3  | 0.0493                        | 0.2144                        | 0.2219                      | 0.4630                      |
| 0.4  | 0.0938                        | 0.3235                        | 0.3063                      | 0.5688                      |
| 0.5  | 0.1577                        | 0.4369                        | 0.3971                      | 0.6610                      |
| 0.6  | 0.2455                        | 0.5516                        | 0.4955                      | 0.7427                      |
| 0.7  | 0.3635                        | 0.6661                        | 0.6029                      | 0.8161                      |
| 0.8  | 0.5199                        | 0.7793                        | 0.7210                      | 0.8828                      |
| 0.9  | 0.7264                        | 0.8907                        | 0.8523                      | 0.9438                      |

The quantile values of the  $\mathcal{PCB}(\alpha, \lambda)$  distribution fall into  $[0, 1]$  for different parameter values. On the other hand, based on the qf, advanced quantile modeling can be performed. For more information, see [10].

### 3. MOMENTS

The moment measures of the  $\mathcal{PCB}(\alpha, \lambda)$  distribution are of interest to describe it in an in-depth manner in terms of central, dispersion, and form parameters, and reveal some statistical features.

The following proposition is about the mathematical expressions of the moments of a random variable following the  $\mathcal{PCB}(\alpha, \lambda)$  distribution.

**Proposition 1.** Let  $Y$  be a random variable following the  $\mathcal{PCB}(\alpha, \lambda)$  distribution and  $m$  be an integer. Then the  $m$ -th moment (or raw moment) of  $Y$  is given by

$$\mathfrak{M}_m = E(Y^m) = \begin{cases} \frac{\alpha}{\alpha + m'} (1 - \lambda)c_\lambda \gamma_- \left[ \frac{m}{\alpha} + 1, 2 \operatorname{arctanh}(1 - 2\lambda) \right], & \lambda = \frac{1}{2}, \\ \frac{(1 - \lambda)c_\lambda}{[2 \operatorname{arctanh}(1 - 2\lambda)]^{m/\alpha + 1}} \gamma_- \left[ \frac{m}{\alpha} + 1, 2 \operatorname{arctanh}(1 - 2\lambda) \right], & \lambda \in \left( 0, \frac{1}{2} \right), \\ \frac{(1 - \lambda)c_\lambda}{[-2 \operatorname{arctanh}(1 - 2\lambda)]^{m/\alpha + 1}} \gamma_+ \left[ \frac{m}{\alpha} + 1, -2 \operatorname{arctanh}(1 - 2\lambda) \right], & \lambda \in \left( \frac{1}{2}, 1 \right), \end{cases}$$

where

$$\gamma_-(x, u) = \int_0^u t^{x-1} e^{-t} dt, \quad \gamma_+(x, u) = \int_0^u t^{x-1} e^t dt. \tag{7}$$

**Proof.** For the case  $\lambda = 1/2$ , we have

$$\mathfrak{M}_m = \int_{-\infty}^{+\infty} x^m f(x; \alpha, \lambda) dx = \alpha \int_0^1 x^m x^{\alpha-1} dx = \frac{\alpha}{\alpha + m}.$$

For the case  $\lambda \in (0, 1) \setminus \{1/2\}$ , by introducing a random variable  $X$  with the  $\mathcal{CB}(\lambda)$  distribution, we have

$$\mathfrak{M}_m = E(X^{m/\alpha}) = \int_{-\infty}^{+\infty} x^{m/\alpha} f(x; \lambda) dx = c_\lambda \int_0^1 x^{m/\alpha} \lambda^x (1 - \lambda)^{1-x} dx.$$

Since  $m/\alpha$  is not necessarily an integer, let us distinguish the case  $\lambda \in (0, 1/2)$  and the case  $\lambda \in (1/2, 1)$ .

- In the case  $\lambda \in (0, 1/2)$ , by applying the change of variable  $y = 2 \operatorname{arctanh}(1 - 2\lambda)x \geq 0$ , we obtain

$$\begin{aligned} \mathfrak{M}_m &= c_\lambda \int_0^1 x^{m/\alpha} e^{x \ln(\lambda) + (1-x) \ln(1-\lambda)} dx = (1-\lambda)c_\lambda \int_0^1 x^{m/\alpha} e^{-x[2 \operatorname{arctanh}(1-2\lambda)]} dx \\ &= \frac{(1-\lambda)c_\lambda}{[2 \operatorname{arctanh}(1-2\lambda)]^{m/\alpha+1}} \int_0^{2 \operatorname{arctanh}(1-2\lambda)} y^{m/\alpha} e^{-y} dy \\ &= \frac{(1-\lambda)c_\lambda}{[2 \operatorname{arctanh}(1-2\lambda)]^{m/\alpha+1}} \gamma_- \left[ \frac{m}{\alpha} + 1, 2 \operatorname{arctanh}(1-2\lambda) \right]. \end{aligned}$$

- In the case  $\lambda \in (1/2, 1)$ , we must take into account a sign detail; by applying the change of variable  $y = -2 \operatorname{arctanh}(1 - 2\lambda)x \geq 0$ , we obtain

$$\begin{aligned} \mathfrak{M}_m &= c_\lambda \int_0^1 x^{m/\alpha} e^{x \ln(\lambda) + (1-x) \ln(1-\lambda)} dx = (1-\lambda)c_\lambda \int_0^1 x^{m/\alpha} e^{-x[2 \operatorname{arctanh}(1-2\lambda)]} dx \\ &= \frac{(1-\lambda)c_\lambda}{[-2 \operatorname{arctanh}(1-2\lambda)]^{m/\alpha+1}} \int_0^{-2 \operatorname{arctanh}(1-2\lambda)} y^{m/\alpha} e^y dy \\ &= \frac{(1-\lambda)c_\lambda}{[-2 \operatorname{arctanh}(1-2\lambda)]^{m/\alpha+1}} \gamma_+ \left[ \frac{m}{\alpha} + 1, -2 \operatorname{arctanh}(1-2\lambda) \right]. \end{aligned}$$

The desired expressions are obtained, ending the proof. □

It is worth noting that the integral function  $\gamma_-(x, u)$  corresponds to the lower incomplete gamma function, which is implemented in most of the mathematical software.

In the case  $\alpha = 1$ ,  $m/\alpha$  is an integer, and we have

$$\mathfrak{M}_m = \begin{cases} \frac{1}{m+1}, & \lambda = \frac{1}{2}, \\ \frac{(1-\lambda)c_\lambda}{[2 \operatorname{arctanh}(1-2\lambda)]^{m+1}} \gamma_- [m+1, 2 \operatorname{arctanh}(1-2\lambda)], & \lambda \in (0, 1) / \left\{ \frac{1}{2} \right\}, \end{cases}$$

giving the  $m$ -th moment related to the  $\mathcal{CB}(\alpha, \lambda)$  distribution, which missing in the list of properties in [19]. In this particular case, by using the expression  $\gamma_-(2, u) = 1 - (1+u)e^{-u}$ , we refine the mean of  $Y$  as precised in [19, Equation (8)]:

$$\mathfrak{M}_1 = \begin{cases} \frac{1}{2}, & \lambda = \frac{1}{2}, \\ \frac{(1-\lambda)c_\lambda}{[2 \operatorname{arctanh}(1-2\lambda)]^2} \gamma_- [2, 2 \operatorname{arctanh}(1-2\lambda)] \\ = \frac{\lambda}{2\lambda-1} + \frac{1}{2 \operatorname{arctanh}(1-2\lambda)}, & \lambda \in (0, 1) / \left\{ \frac{1}{2} \right\}. \end{cases}$$

More generally, based on the expression of the moments established in Proposition 1, we can easily derive the mean of a random variable  $Y$  following the  $\mathcal{PCB}(\alpha, \lambda)$  distribution; it is given as

$$\mathfrak{M}_1 = \begin{cases} \frac{\alpha}{\alpha+1}, & \lambda = \frac{1}{2}, \\ \frac{(1-\lambda)c_\lambda}{[2 \operatorname{arctanh}(1-2\lambda)]^{1/\alpha+1}} \gamma_- \left[ \frac{1}{\alpha} + 1, 2 \operatorname{arctanh}(1-2\lambda) \right], & \lambda \in \left( 0, \frac{1}{2} \right), \\ \frac{(1-\lambda)c_\lambda}{[-2 \operatorname{arctanh}(1-2\lambda)]^{1/\alpha+1}} \gamma_+ \left[ \frac{1}{\alpha} + 1, -2 \operatorname{arctanh}(1-2\lambda) \right], & \lambda \in \left( \frac{1}{2}, 1 \right), \end{cases}$$

as well the moment of order 2 of  $Y$ :

$$\mathfrak{M}_2 = \begin{cases} \frac{\alpha}{\alpha+2}, & \lambda = \frac{1}{2}, \\ \frac{(1-\lambda)c_\lambda}{[2 \operatorname{arctanh}(1-2\lambda)]^{2/\alpha+1}} \gamma_- \left[ \frac{2}{\alpha} + 1, 2 \operatorname{arctanh}(1-2\lambda) \right], & \lambda \in \left( 0, \frac{1}{2} \right), \\ \frac{(1-\lambda)c_\lambda}{[-2 \operatorname{arctanh}(1-2\lambda)]^{2/\alpha+1}} \gamma_+ \left[ \frac{2}{\alpha} + 1, -2 \operatorname{arctanh}(1-2\lambda) \right], & \lambda \in \left( \frac{1}{2}, 1 \right). \end{cases}$$

The variance of  $Y$  follows from the standard formula:  $\sigma^2 = \mathfrak{M}_2 - \mathfrak{M}_1^2$ . The  $m$ -th central moment of  $Y$  is given by

$$\mathfrak{M}_m^* = E[(Y - \mathfrak{M}_1)^m] = \sum_{k=0}^m \binom{m}{k} (-1)^{m-k} \mathfrak{M}_k \mathfrak{M}_1^{m-k}.$$

Based on these central moments, the skewness and kurtosis coefficients of  $Y$  are, respectively, given by

$$S = \frac{\mathfrak{M}_3^*}{\sigma^3}, \quad K = \frac{\mathfrak{M}_4^*}{\sigma^4}.$$

Numerical computation of the mean, variance, measures of skewness and kurtosis for the  $\mathcal{PCB}(\alpha, \lambda)$  distribution are shown in Table 2.

**Table 2:** Theoretical moment measures of the  $\mathcal{PCB}(\alpha, \lambda)$  distribution

| $\alpha$ | $\lambda$ | $\mathfrak{M}_1$ | $\sigma^2$ | $S$     | $K$    |
|----------|-----------|------------------|------------|---------|--------|
| 0.5      | 0.1       | 0.1755           | 0.0528     | 1.6646  | 5.0278 |
|          | 0.4       | 0.3001           | 0.0837     | 0.8087  | 2.4314 |
|          | 0.9       | 0.5152           | 0.0923     | -0.1377 | 1.7674 |
| 1.0      | 0.1       | 0.3301           | 0.0665     | 0.7430  | 2.5785 |
|          | 0.4       | 0.4663           | 0.0827     | 0.1417  | 1.8116 |
|          | 0.9       | 0.6699           | 0.0664     | -0.7388 | 2.5633 |
| 2.0      | 0.1       | 0.5234           | 0.0562     | 0.0559  | 2.0882 |
|          | 0.4       | 0.6394           | 0.0575     | -0.4382 | 2.2506 |
|          | 0.9       | 0.7962           | 0.0360     | -1.3390 | 4.3644 |

From Table 2, we conclude that the  $\mathcal{PCB}(\alpha, \lambda)$  distribution can be left- and right-skewed, as negative and positive values for  $S$  are observed, and it has all kurtosis states, as  $K$  varies around the limit value of 3.

**Complement:** Alternative measures of skewness and kurtosis are the ones based on the qf of the distribution as proposed by [7] and [22], respectively. The Galton skewness and the Moors kurtosis are, respectively, defined as

$$S_G = \frac{Q(6/8; \alpha, \lambda) - 2Q(4/8; \alpha, \lambda) + Q(2/8; \alpha, \lambda)}{Q(6/8; \alpha, \lambda) - Q(2/8; \alpha, \lambda)}$$

and

$$K_M = \frac{Q(7/8; \alpha, \lambda) - Q(5/8; \alpha, \lambda) + Q(3/8; \alpha, \lambda) - Q(1/8; \alpha, \lambda)}{Q(6/8; \alpha, \lambda) - Q(2/8; \alpha, \lambda)}.$$

In order to complete the previous numerical work, Figure 3 presents the nature of the Galton skewness and Moors kurtosis of the  $\mathcal{PCB}(\alpha, \lambda)$  distribution.

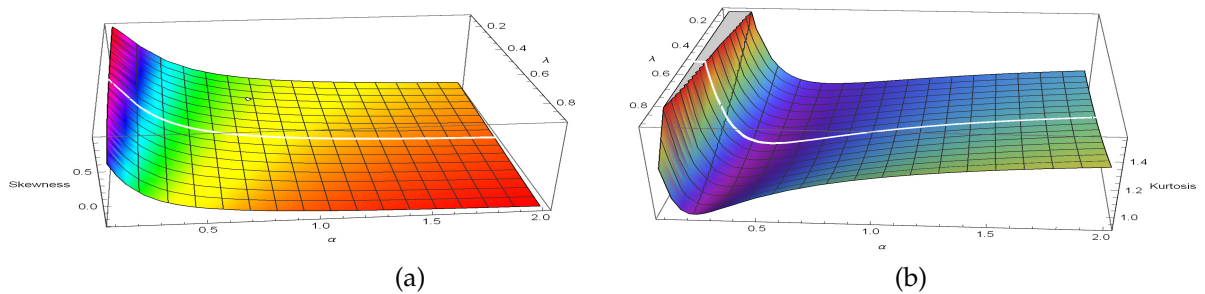


**Figure 3:** Plots of (a) the Galton skewness and (b) Moors kurtosis for the  $\mathcal{PCB}(\alpha, \lambda)$  distribution with  $\alpha \in [0, 2]$  and  $\lambda \in [0, 1]$

From Figure 3, we can observe that the Galton skewness seems monotonic according to  $\alpha$  and  $\lambda$ , with possible negative and positive values. On the other hand, the Moors kurtosis is more complex, being non-monotonic in  $\alpha$ . This illustrates the versatility of the  $\mathcal{PCB}(\alpha, \lambda)$  distribution on these form aspects.

#### 4. ENTROPY

The amount of randomness in the  $\mathcal{PCB}(\alpha, \lambda)$  distribution is now the object of all the attention. In order to accomplish this, we recall that the Rényi entropy of a random variable  $X$  with pdf  $f(x)$  is given by

$$\mathfrak{R}_\theta = \frac{1}{1-\theta} \ln \left[ \int_{-\infty}^{+\infty} f(x)^\theta dx \right],$$

with  $\theta > 0$  and  $\theta \neq 1$ . The following proposition is about the mathematical expression of the Rényi entropy of a random variable  $Y$  following the  $\mathcal{PCB}(\alpha, \lambda)$  distribution.

**Proposition 2.** Let  $\theta > 0$  with  $\theta \neq 1$ , and  $Y$  be a random variable following the  $\mathcal{PCB}(\alpha, \lambda)$  distribution. Then the Rényi entropy of  $Y$  is given by

$$\mathfrak{R}_\theta = \begin{cases} \frac{1}{1-\theta} \ln \left( \frac{\alpha^\theta}{\theta(\alpha-1)+1} \right), & \lambda = \frac{1}{2}, \\ \frac{1}{1-\theta} \ln \left\{ \frac{(1-\lambda)^\theta c_\lambda^\theta \alpha^{\theta-1}}{[2\theta \operatorname{arctanh}(1-2\lambda)]^{(\theta-1)(\alpha-1)/\alpha+1}} \gamma_- \left[ \frac{(\theta-1)(\alpha-1)}{\alpha} + 1, 2\theta \operatorname{arctanh}(1-2\lambda) \right] \right\}, & \lambda \in \left(0, \frac{1}{2}\right), \\ \frac{1}{1-\theta} \ln \left\{ \frac{(1-\lambda)^\theta c_\lambda^\theta \alpha^{\theta-1}}{[-2\theta \operatorname{arctanh}(1-2\lambda)]^{(\theta-1)(\alpha-1)/\alpha+1}} \gamma_+ \left[ \frac{(\theta-1)(\alpha-1)}{\alpha} + 1, -2\theta \operatorname{arctanh}(1-2\lambda) \right] \right\}, & \lambda \in \left(\frac{1}{2}, 1\right), \end{cases}$$

where  $\gamma_-(x, u)$  and  $\gamma_+(x, u)$  are defined as in (7).

**Proof.** For the case  $\lambda = 1/2$ , we have

$$\int_{-\infty}^{+\infty} f(x; \alpha, \lambda)^\theta dx = \alpha^\theta \int_0^1 x^{\theta(\alpha-1)} dx = \frac{\alpha^\theta}{\theta(\alpha-1)+1}.$$

Hence,

$$\mathfrak{R}_\theta = \frac{1}{1-\theta} \ln \left( \frac{\alpha^\theta}{\theta(\alpha-1)+1} \right).$$

For the case  $\lambda \in (0, 1) \setminus \{1/2\}$ , by applying the change of variable  $y = x^\alpha$ , we have

$$\begin{aligned} \int_{-\infty}^{+\infty} f(x; \alpha, \lambda)^\theta dx &= c_\lambda^\theta \alpha^\theta \int_0^1 x^{\theta(\alpha-1)} \lambda^{\theta x^\alpha} (1-\lambda)^{\theta(1-x^\alpha)} dx \\ &= c_\lambda^\theta \alpha^{\theta-1} \int_0^1 y^{(\theta-1)(\alpha-1)/\alpha} \lambda^{\theta y} (1-\lambda)^{\theta(1-y)} dy. \end{aligned}$$

Let us now distinguish the case  $\lambda \in (0, 1/2)$  and the case  $\lambda \in (1/2, 1)$ .

- In the case  $\lambda \in (0, 1/2)$ , by applying the change of variable  $t = 2\theta \operatorname{arctanh}(1-2\lambda)y \geq 0$ , we obtain

$$\begin{aligned} \int_{-\infty}^{+\infty} f(x; \alpha, \lambda)^\theta dx &= c_\lambda^\theta \alpha^{\theta-1} \int_0^1 y^{(\theta-1)(\alpha-1)/\alpha} e^{\theta y \ln(\lambda) + \theta(1-y) \ln(1-\lambda)} dy \\ &= (1-\lambda)^\theta c_\lambda^\theta \alpha^{\theta-1} \int_0^1 y^{(\theta-1)(\alpha-1)/\alpha} e^{-y[2\theta \operatorname{arctanh}(1-2\lambda)]} dy \\ &= \frac{(1-\lambda)^\theta c_\lambda^\theta \alpha^{\theta-1}}{[2\theta \operatorname{arctanh}(1-2\lambda)]^{(\theta-1)(\alpha-1)/\alpha+1}} \int_0^{2\theta \operatorname{arctanh}(1-2\lambda)} t^{(\theta-1)(\alpha-1)/\alpha} e^{-t} dt \\ &= \frac{(1-\lambda)^\theta c_\lambda^\theta \alpha^{\theta-1}}{[2\theta \operatorname{arctanh}(1-2\lambda)]^{(\theta-1)(\alpha-1)/\alpha+1}} \gamma_- \left[ \frac{(\theta-1)(\alpha-1)}{\alpha} + 1, 2\theta \operatorname{arctanh}(1-2\lambda) \right]. \end{aligned}$$

Hence,

$$\mathfrak{R}_\theta = \frac{1}{1-\theta} \ln \left\{ \frac{(1-\lambda)^\theta c_\lambda^\theta \alpha^{\theta-1}}{[2\theta \operatorname{arctanh}(1-2\lambda)]^{(\theta-1)(\alpha-1)/\alpha+1}} \gamma_- \left[ \frac{(\theta-1)(\alpha-1)}{\alpha} + 1, 2\theta \operatorname{arctanh}(1-2\lambda) \right] \right\}.$$

- In the case  $\lambda \in (1/2, 1)$ , by applying the change of variable  $t = -2\theta \operatorname{arctanh}(1 - 2\lambda)y \geq 0$ , we obtain

$$\begin{aligned} \int_{-\infty}^{+\infty} f(x; \alpha, \lambda)^\theta dx &= c_\lambda^\theta \alpha^{\theta-1} \int_0^1 y^{(\theta-1)(\alpha-1)/\alpha} e^{\theta y \ln(\lambda) + \theta(1-y) \ln(1-\lambda)} dy \\ &= (1-\lambda)^\theta c_\lambda^\theta \alpha^{\theta-1} \int_0^1 y^{(\theta-1)(\alpha-1)/\alpha} e^{-y[2\theta \operatorname{arctanh}(1-2\lambda)]} dy \\ &= \frac{(1-\lambda)^\theta c_\lambda^\theta \alpha^{\theta-1}}{[-2\theta \operatorname{arctanh}(1-2\lambda)]^{(\theta-1)(\alpha-1)/\alpha+1}} \int_0^{-2\theta \operatorname{arctanh}(1-2\lambda)} t^{(\theta-1)(\alpha-1)/\alpha} e^t dt \\ &= \frac{(1-\lambda)^\theta c_\lambda^\theta \alpha^{\theta-1}}{[-2\theta \operatorname{arctanh}(1-2\lambda)]^{(\theta-1)(\alpha-1)/\alpha+1}} \gamma_+ \left[ \frac{(\theta-1)(\alpha-1)}{\alpha} + 1, -2\theta \operatorname{arctanh}(1-2\lambda) \right]. \end{aligned}$$

Hence,

$$\mathfrak{R}_\theta = \frac{1}{1-\theta} \ln \left\{ \frac{(1-\lambda)^\theta c_\lambda^\theta \alpha^{\theta-1}}{[-2\theta \operatorname{arctanh}(1-2\lambda)]^{(\theta-1)(\alpha-1)/\alpha+1}} \gamma_+ \left[ \frac{(\theta-1)(\alpha-1)}{\alpha} + 1, -2\theta \operatorname{arctanh}(1-2\lambda) \right] \right\}.$$

We end the proof by compiling the above expressions. □

Table 3 shows some numerical values of the Rényi entropy of the  $\mathcal{PCB}(\alpha, \lambda)$  distribution.

**Table 3:** Numerical results of the Rényi entropy of the  $\mathcal{PCB}(\alpha, \lambda)$  distribution

| $\gamma$ | $\alpha = 1, \lambda = 0.3$ | $\alpha = 1, \lambda = 0.8$ | $\alpha = 2, \lambda = 0.3$ | $\alpha = 2, \lambda = 0.8$ |
|----------|-----------------------------|-----------------------------|-----------------------------|-----------------------------|
| 0.01     | -0.0003                     | -0.0008                     | -0.0019                     | -0.0061                     |
| 0.03     | -0.0009                     | -0.0024                     | -0.0057                     | -0.0813                     |
| 0.5      | -0.0148                     | -0.0390                     | -0.0712                     | -0.2523                     |
| 0.7      | -0.0207                     | -0.0542                     | -0.0901                     | -0.3290                     |
| 2.0      | -0.0574                     | -0.1443                     | -0.1604                     | -0.6414                     |
| 4.0      | -0.1069                     | -0.2468                     | -0.2056                     | -0.8486                     |
| 7.0      | -0.1624                     | -0.3379                     | -0.2360                     | -0.9827                     |
| 9.0      | -0.1892                     | -0.3756                     | -0.2474                     | -1.0320                     |

Consequently, from Table 3, some useful properties of the Rényi entropy provided in [11] are applicable here. In particular, (i) for any  $\theta_1 < \theta_2$ , we have  $\mathfrak{R}_{\theta_2} \leq \mathfrak{R}_{\theta_1}$ , (ii) the Rényi entropy can be negative.

## 5. STATISTICAL APPLICATIONS

This section is devoted to the applicability of the  $\mathcal{PCB}(\alpha, \lambda)$  distribution.

### 5.1. Estimation

In the setting of the  $\mathcal{PCB}(\alpha, \lambda)$  distribution, we aim to estimate the unknown parameters  $\alpha$  and  $\lambda$  based on data that can be conceptually fitted with this distribution. To accomplish this, we can use the ML method, described as follows: Let  $y_1, \dots, y_n$  represent  $n$  independent observations from a random variable  $Y$  following the  $\mathcal{PCB}(\alpha, \lambda)$  distribution. Then, based on the pdf indicated

in (5), the likelihood function is specified by

$$L(\alpha, \lambda; y_1, \dots, y_n) = \prod_{i=1}^n f(y_i; \alpha, \lambda)$$

$$= \begin{cases} \alpha^n \left[ \prod_{i=1}^n y_i \right]^{\alpha-1}, & \lambda = \frac{1}{2}, \\ c_\lambda^n \alpha^n \left[ \prod_{i=1}^n y_i \right]^{\alpha-1} \lambda^{\sum_{i=1}^n y_i^\alpha} (1-\lambda)^{n-\sum_{i=1}^n y_i^\alpha}, & \lambda \in (0, 1) / \left\{ \frac{1}{2} \right\}. \end{cases}$$

The ML estimates (MLEs) of  $\alpha$  and  $\lambda$  are given by

$$(\hat{\alpha}, \hat{\lambda}) = \operatorname{argmax}_{(\alpha, \lambda)} L(\alpha, \lambda; y_1, \dots, y_n).$$

Alternatively, they are defined by

$$(\hat{\alpha}, \hat{\lambda}) = \operatorname{argmax}_{(\alpha, \lambda)} \ell(\alpha, \lambda; y_1, \dots, y_n),$$

where  $\ell(\alpha, \lambda; y_1, \dots, y_n)$  refers to the log-likelihood function given by

$$\ell(\alpha, \lambda; y_1, \dots, y_n) = \ln [L(\alpha, \lambda; y_1, \dots, y_n)]$$

$$= \begin{cases} n \ln(\alpha) + (\alpha - 1) \sum_{i=1}^n \ln(y_i), & \lambda = \frac{1}{2}, \\ n \ln(c_\lambda) + n \ln(\alpha) + (\alpha - 1) \sum_{i=1}^n \ln(y_i) + \ln(\lambda) \sum_{i=1}^n y_i^\alpha + \ln(1-\lambda) \left[ n - \sum_{i=1}^n y_i^\alpha \right], & \lambda \in (0, 1) / \left\{ \frac{1}{2} \right\}. \end{cases}$$

They can be obtained by solving the following non-linear equations with respect to  $\alpha$  and  $\lambda$ :

$$\frac{\partial \ell(\alpha, \lambda; y_1, \dots, y_n)}{\partial \alpha} = 0, \quad \frac{\partial \ell(\alpha, \lambda; y_1, \dots, y_n)}{\partial \lambda} = 0.$$

The standard errors of  $\hat{\alpha}$  and  $\hat{\lambda}$  can be approximated, and they are denoted in the next as  $se(\hat{\alpha})$  and  $se(\hat{\lambda})$ , respectively. The advantage of the ML method is that it guarantees interesting properties for the MLEs, such as asymptotic unbiasedness and normality. More information on these properties can be found in [4]. Based on the MLEs, we can estimate all the underlying functions of the  $\mathcal{PCB}(\alpha, \lambda)$  distribution. In particular, an estimate of the cdf  $F(x; \alpha, \lambda)$  is given by  $\hat{F}(x) = F(x; \hat{\alpha}, \hat{\lambda})$  and an estimate of the pdf  $f(x; \alpha, \lambda)$  is given by  $\hat{f}(x) = f(x; \hat{\alpha}, \hat{\lambda})$ .

## 5.2. Simulation study

In this portion, we investigate the asymptotic behavior of the MLEs of  $\alpha$  and  $\lambda$  using Monte Carlo simulation. Random samples from the  $\mathcal{PCB}(\alpha, \lambda)$  distribution were generated using (6). The simulation is repeated  $N = 2000$  times for different sample sizes  $n \in \{20, 50, 100, 200, 500\}$  and different choices of the parameter values  $(\alpha = 0.3, \lambda = 0.1)$ ,  $(\alpha = 0.5, \lambda = 0.3)$  and  $(\alpha = 0.8, \lambda = 0.6)$ . The performance of the MLEs is examined using various statistical criteria presented below. For  $\phi \in \{\alpha, \lambda\}$ , we consider

1. the average bias (Bias) defined by  $\frac{1}{N} \sum_{i=1}^N (\hat{\phi}_i - \phi)$ , where the index  $i$  refers to the  $i$ -th experiment among the  $N$ ,

2. the root mean square error (RMSE) defined by  $\sqrt{\frac{1}{N} \sum_{i=1}^N (\hat{\phi}_i - \phi)^2}$ ,

3. the coverage probability (CP) of the 95% confidence interval defined by

$$\frac{1}{N} \sum_{i=1}^N I(\hat{\phi}_i - u_* se(\hat{\phi}_i) < \phi < \hat{\phi}_i + u_* se(\hat{\phi}_i)),$$

where  $I(\cdot)$  is the indicator function,  $se(\hat{\phi}_i)$  is the standard error related to  $\hat{\phi}_i$  and  $u_* = 1.959964$ . Table 4 presents the simulation results based on these criteria.

**Table 4:** Simulation results for the unknown parameters estimates of  $\mathcal{PCB}(\alpha, \lambda)$  distribution

| Parameters                        | $n$ | Bias     |           | RMSE     |           | CP       |           |
|-----------------------------------|-----|----------|-----------|----------|-----------|----------|-----------|
|                                   |     | $\alpha$ | $\lambda$ | $\alpha$ | $\lambda$ | $\alpha$ | $\lambda$ |
| $\alpha = 0.3$<br>$\lambda = 0.1$ | 25  | 0.0189   | 0.0234    | 0.0807   | 0.1314    | 0.9420   | 0.8065    |
|                                   | 50  | 0.0056   | 0.0156    | 0.0520   | 0.0934    | 0.9455   | 0.8425    |
|                                   | 100 | 0.0042   | 0.0062    | 0.0358   | 0.0565    | 0.9570   | 0.9000    |
|                                   | 200 | 0.0028   | 0.0028    | 0.0255   | 0.0406    | 0.9450   | 0.9060    |
|                                   | 500 | 0.0006   | 0.0014    | 0.0155   | 0.0250    | 0.9520   | 0.9395    |
| $\alpha = 0.5$<br>$\lambda = 0.3$ | 25  | 0.0528   | -0.0061   | 0.1736   | 0.2073    | 0.9440   | 0.8120    |
|                                   | 50  | 0.0228   | -0.0040   | 0.1139   | 0.1608    | 0.9545   | 0.8675    |
|                                   | 100 | 0.0095   | 0.0075    | 0.0819   | 0.1251    | 0.9470   | 0.9150    |
|                                   | 200 | 0.0037   | 0.0040    | 0.0554   | 0.0902    | 0.9515   | 0.9300    |
|                                   | 500 | 0.0029   | -0.0002   | 0.0341   | 0.0569    | 0.9575   | 0.9405    |
| $\alpha = 0.8$<br>$\lambda = 0.6$ | 25  | 0.1847   | -0.1243   | 0.3970   | 0.2635    | 0.9485   | 0.8380    |
|                                   | 50  | 0.0959   | -0.0711   | 0.2636   | 0.2073    | 0.9420   | 0.8835    |
|                                   | 100 | 0.0460   | -0.0380   | 0.1832   | 0.1628    | 0.9445   | 0.9090    |
|                                   | 200 | 0.0189   | -0.0155   | 0.1276   | 0.1221    | 0.9620   | 0.9285    |
|                                   | 500 | 0.0065   | -0.0051   | 0.0827   | 0.0818    | 0.9540   | 0.9365    |

From Table 4, we notice that the RMSE of both MLEs decreases as the sample size  $n$  increases. While  $\hat{\alpha}$  is a positively biased parameter estimate,  $\hat{\lambda}$  can be both positively and negatively biased. Furthermore, the CP of both MLEs approaches 0.95, and the CP of  $\lambda$  increases as the sample size  $n$  increases.

### 5.3. Real-life data fitting

Among other purposes, the  $\mathcal{PCB}(\alpha, \lambda)$  distribution can be used for fitting data with values into  $[0, 1]$ . We thus illustrate this application by considering two real-life data sets, and compare their fit with the ones obtained from some existing distributions with support of  $[0, 1]$ . More specifically, we consider the following recently developed unit distributions, including the beta and Kumaraswamy distributions.

1. Marshall-Olkin extended Kumaraswamy distribution (MOEKD) introduced by [8], and defined with the following pdf:

$$f(x; \alpha, a, b) = \frac{\alpha a b x^{a-1} (1-x^a)^{b-1}}{[1 - \bar{\alpha} (1-x^a)^b]^2}, \quad x \in [0, 1], \text{ where } \bar{\alpha} = 1 - \alpha, \text{ with } \alpha, a, b > 0.$$

2. Marshall-Olkin extended Topp-Leone distribution (MOETLD) introduced by [25], and specified by the following pdf:

$$f(x; \alpha, \lambda) = \frac{2\alpha\lambda(1-x) [1 - (1-x)^2]^{\lambda-1}}{[1 - \bar{\alpha} (1 - [1 - (1-x)^2]^\lambda)]^2}, \quad x \in [0, 1], \text{ with } \alpha, \lambda > 0.$$

3. Unit-Gompertz distribution (UGD) introduced by [20], and defined with the following pdf:

$$f(x; a, b) = abx^{-a-1}e^{-b(x^{-a}-1)}, \quad x \in (0, 1], \text{ with } a, b > 0.$$

4. Unit-Burr XII distribution (UBXIID) introduced by [16], and defined with the following pdf:

$$f(x; \alpha, \beta) = \alpha\beta x^{-1}(-\ln(x))^{\beta-1} (1 + (-\ln(x))^\beta)^{-\alpha-1}, \quad x \in (0, 1], \text{ with } \alpha, \beta > 0.$$

5. Kumaraswamy distribution introduced by [17], and characterized by the following pdf:  
 $f(x; a, b) = abx^{a-1}(1-x)^b, \quad x \in (0, 1],$  with  $a, b > 0$ .
6. Beta distribution reported in [24], and defined with the following pdf:  
 $f(x; \alpha, \beta) = \frac{\Gamma(\alpha + \beta)}{\Gamma(\alpha)\Gamma(\beta)} x^{\alpha-1}(1-x)^{\beta-1}, \quad x \in (0, 1),$  where  $\Gamma(x)$  refers to the standard gamma function, with  $\alpha, \beta > 0$ .
7. Continuous Bernoulli distribution (CBD) reported in [30], and defined with the pdf given in (1).

For clarity in exposition, we finally mention that the  $\mathcal{PCB}(\alpha, \lambda)$  distribution will sometimes be denoted as PCB in the figures and tables to come.

**Data set 1:** The first data set consists of trade share data from [3]. The trade share data are as follows: 0.140501976, 0.156622976, 0.157703221, 0.160405084, 0.160815045, 0.22145839, 0.299405932, 0.31307286, 0.324612707, 0.324745566, 0.329479247, 0.330021679, 0.337879002, 0.339706242, 0.352317631, 0.358856708, 0.393250912, 0.41760394, 0.425837249, 0.43557933, 0.442142904, 0.444374621, 0.450546652, 0.4557693, 0.46834656, 0.473254889, 0.484600782, 0.488949597, 0.509590268, 0.517664552, 0.527773321, 0.534684658, 0.543337107, 0.544243515, 0.550812602, 0.552722335, 0.56064254, 0.56074965, 0.567130983, 0.575274825, 0.582814276, 0.603035331, 0.605031252, 0.613616884, 0.626079738, 0.639484167, 0.646913528, 0.651203632, 0.681555152, 0.699432909, 0.704819918, 0.729232311, 0.742971599, 0.745497823, 0.779847085, 0.798375845, 0.814710021, 0.822956383, 0.830238342, 0.834204197, and 0.979355395. The data set is approximately symmetric with a skewness value of 0.0059. Details of this data set can be accessed in [29].

**Data set 2:** The second data set relates to 30 measurements of the tensile strength of polyester fibers reported in [20]. It was first reported in [27]. The data are as follows: 0.023, 0.032, 0.054, 0.069, 0.081, 0.094, 0.105, 0.127, 0.148, 0.169, 0.188, 0.216, 0.255, 0.277, 0.311, 0.361, 0.376, 0.395, 0.432, 0.463, 0.481, 0.519, 0.529, 0.567, 0.642, 0.674, 0.752, 0.823, 0.887, and 0.926. The data set is right-skewed with a skewness value of 0.5193.

Figure 4 presents the boxplot for the two data sets, showing some of their quantile characteristics.

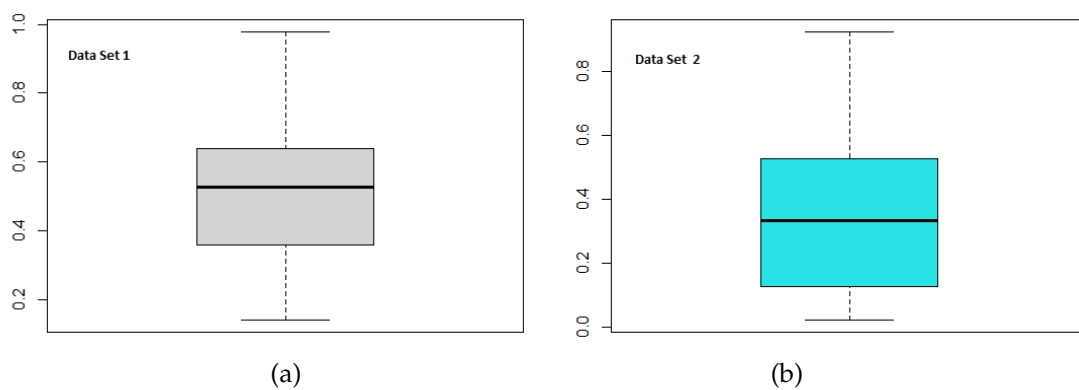


**Figure 4:** Boxplot for (a) data set 1 and (b) data set 2

Figure 4 further supports the claim that data set 1 is approximately symmetric while data set 2 is right-skewed. Observe also that there are no outliers in the two data sets.

The distribution comparison will be based on the distribution parameter estimates, log-likelihood (LogL), Akaike information criterion (AIC), and Kolmogorov-Smirnov test statistic (K-S), along with the corresponding  $p$ -value. Tables 5 and 6 present the summary statistics for data sets 1 and 2, respectively.

**Table 5:** Summary statistics for data set 1

| Models      | Estimates  | LogL    | AIC      | K-S    | <i>p</i> -value |
|-------------|--|---------|----------|--------|-----------------|
| PCBD        | $\alpha = 2.8491$<br>$\lambda = 0.0094$<br>$\alpha = 0.3011$ | 15.1002 | -26.2005 | 0.0565 | 0.9837          |
| MOEKD       | $a = 3.0586$<br>$b = 1.9513$                                 | 14.3183 | -22.6367 | 0.0582 | 0.9783          |
| MOETLD      | $\alpha = 0.6630$<br>$\lambda = 3.3521$                      | 14.3606 | -24.7211 | 0.0568 | 0.9831          |
| Beta        | $\alpha = 2.7940$<br>$\beta = 2.6038$                        | 13.9561 | -23.9121 | 0.1162 | 0.3546          |
| UGD         | $a = 0.6162$<br>$b = 1.0921$                                 | 10.8759 | -17.7518 | 0.1098 | 0.4235          |
| UBXIID      | $\alpha = 2.1247$<br>$\beta = 2.2237$                        | 14.1186 | -24.2371 | 0.0578 | 0.9804          |
| Kumaraswamy | $a = 2.3297$<br>$b = 2.7630$                                 | 13.6251 | -23.2503 | 0.0689 | 0.9142          |
| CBD         | $\lambda = 0.5424$   | 0.0734  | 1.8532   | 0.1834 | 0.0287          |

**Table 6:** Summary statistics for data set 2

| Models      | Estimates  | LogL   | AIC     | K-S    | <i>p</i> -value |
|-------------|--|--------|---------|--------|-----------------|
| PCBD        | $\alpha = 1.1240$<br>$\lambda = 0.1069$<br>$\alpha = 0.4363$ | 3.4469 | -2.8938 | 0.0578 | 0.9998          |
| MOEKD       | $a = 1.1874$<br>$b = 1.2582$                                 | 3.6043 | -1.2088 | 0.0627 | 0.9992          |
| MOETLD      | $\alpha = 1.0929$<br>$\lambda = 1.0628$                      | 2.9136 | -1.8272 | 0.0672 | 0.9978          |
| Beta        | $\alpha = 0.9666$<br>$\beta = 1.6203$                        | 3.3051 | -2.6101 | 0.1646 | 0.3515          |
| UGD         | $a = 1.0373$<br>$b = 0.4213$                                 | 3.9488 | -3.8976 | 0.0734 | 0.9932          |
| UBXIID      | $\alpha = 1.0331$<br>$\beta = 1.8465$                        | 1.0390 | 1.9220  | 0.0993 | 0.9007          |
| Kumaraswamy | $a = 0.9627$<br>$b = 1.6084$                                 | 3.3110 | -2.6221 | 0.0649 | 0.9987          |
| CBD         | $\lambda = 0.1565$   | 3.3118 | -4.6236 | 0.0594 | 0.9997          |

#### 5.4. Discussion of the results

In the model selection concept, the model that best fits the data set is traceable to the one having the maximized LogL, least value in terms of AIC and K-S with the highest *p*-value. A close look at Tables 5 and 6 reveals that the  $\mathcal{PCB}(\alpha, \lambda)$  distribution outperforms the competitors in fitting the two data sets under study. In particular, all the comparison criteria in Table 5 are in favor of the  $\mathcal{PCB}(\alpha, \lambda)$  distribution. Whereas, in Table 6, we observe that LogL as a criterion supports the Marshall-Olkin extended Kumaraswamy and unit-Gompertz distributions over the  $\mathcal{PCB}(\alpha, \lambda)$  distribution, while the AIC supports the unit-Gompertz and continuous Bernoulli distributions over the  $\mathcal{PCB}(\alpha, \lambda)$  distribution. However, the  $\mathcal{PCB}(\alpha, \lambda)$  distribution outperforms all of the

competitors in terms of the K-S statistic and its corresponding p-value. Figures 5,6,7 and 8 show additional evidence of its flexibility over the competitors.

Especially, Figure 5 displays the estimated pdf and cdf fits of the distributions for data set 1.

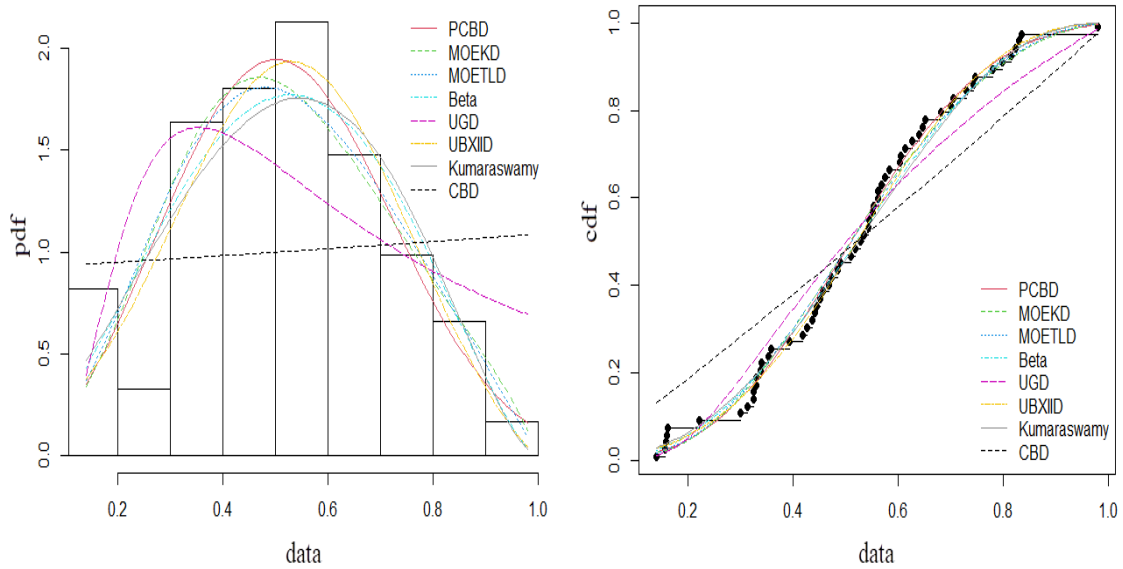


Figure 5: Estimated pdf and cdf fits of the distributions for data set 1

We observe that the estimated pdf fit of the  $PCB(\alpha, \lambda)$  distribution perfectly captures the shape of the unimodal histogram, and the estimated cdf fit approaches well the curvature of the empirical cdf.

In Figure 6 the probability-probability (P-P) plots of the distributions for data set 1 are shown.

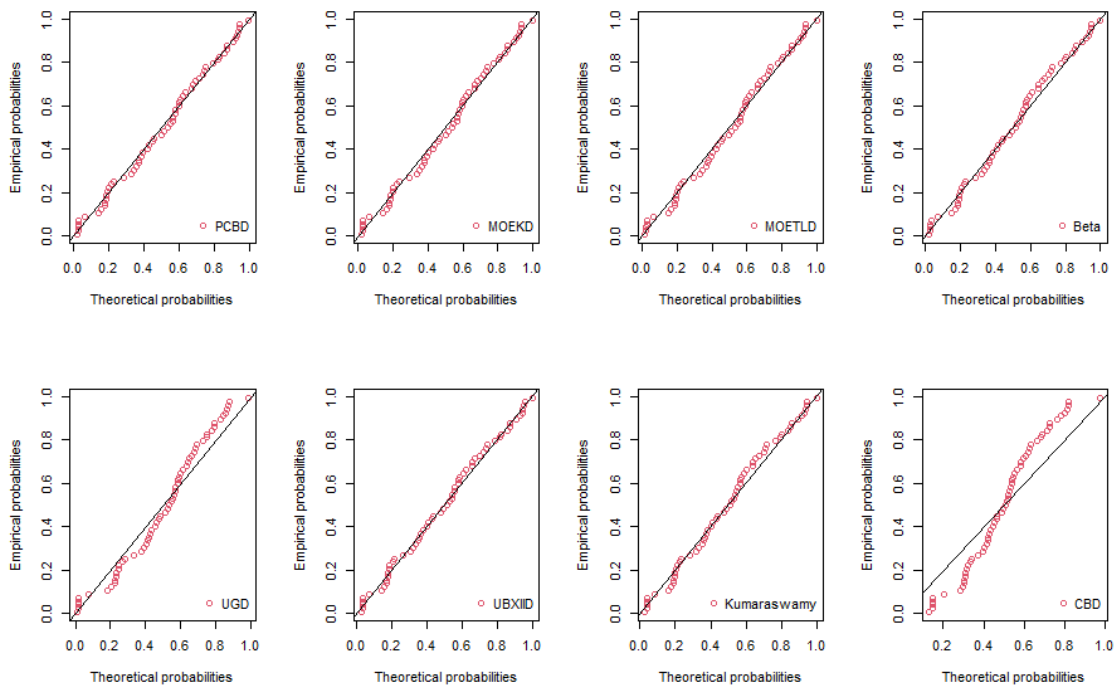


Figure 6: P-P plot of the distributions for data set 1

Visually, the P-P line of the  $\mathcal{PCB}(\alpha, \lambda)$  distribution better adjusts the associated scatter plot than the others.

Figure 7 is analogous to Figure 5 but for data set 2.

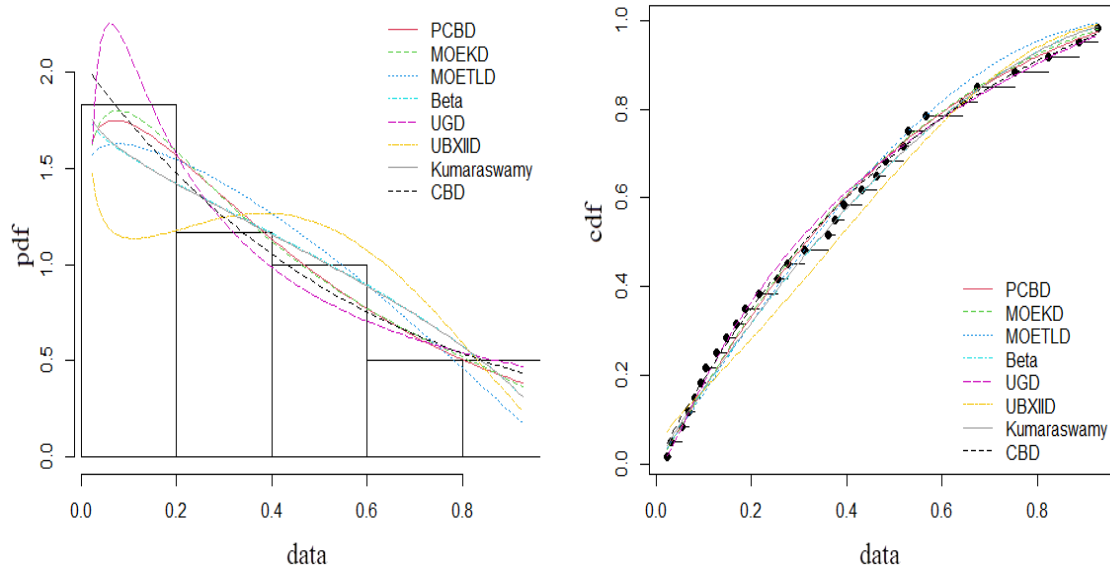


Figure 7: Estimated pdf and cdf fits of the distributions for data set 2

In Figure 7, the estimated pdf fit of the  $\mathcal{PCB}(\alpha, \lambda)$  distribution captures well the decreasing shape of the histogram, and the estimated cdf fit approaches correctly the concave trend of the empirical cdf.

Figure 8 is analogous to Figure 6 but for data set 2.

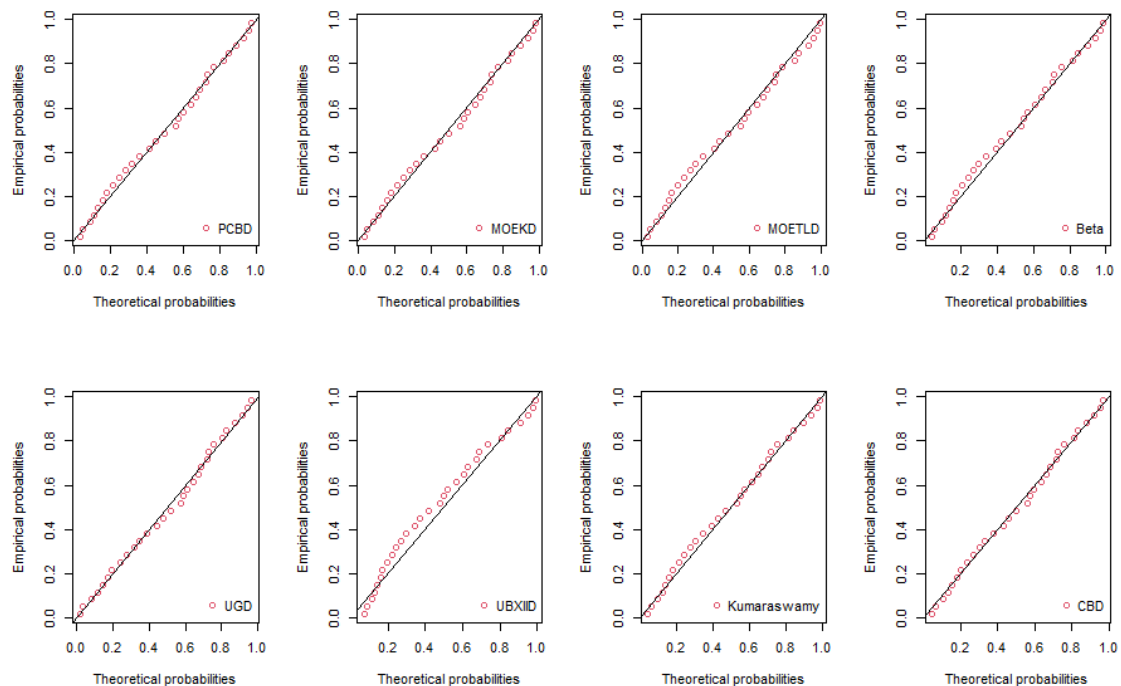


Figure 8: P-P plots of the distributions for data set 2

In Figure 8, the P-P line of the  $\mathcal{PCB}(\alpha, \lambda)$  distribution is quite acceptable in terms of fitting, as for some other competitors.

In summary, from these figures, it is clear that the fit accuracy of the  $\mathcal{PCB}(\alpha, \lambda)$  distribution is excellent, making it a golden distribution to analyze the considered data sets.

## 6. CONCLUSION

We proposed a natural extension of the novel continuous Bernoulli distribution by adding a shape parameter through power transformation. The so-called power continuous Bernoulli distribution is aimed at extending the modeling scope of the continuous Bernoulli distribution. Some of its mathematical properties were derived (moments, quantiles, entropy, etc.). A parametric estimation exercise has been given through the maximum likelihood method, and the asymptotic behavior of the parameter estimates was investigated through a Monte Carlo simulation study. Finally, we illustrate the flexibility of the power continuous Bernoulli distribution in real-life data fitting using two real data sets. The potential for probability and statistics applications, such as regression modeling and machine learning applications, is enormous, and this study provides the first steps in that direction.

## Conflict of Interests

The authors declare that there are no conflicts of interest regarding the publication of this paper.

## REFERENCES

- [1] Altun, E. (2018). The log-xgamma distribution with inference and application. *Journal de la Société de Statistique de Paris*, 159(3): 40-55.
- [2] Bantan, R. A. R., Chesneau, C. and Jamal, F. (2020). Some new facts about the unit-Rayleigh distribution with applications. *Mathematics*, 8(11): 1-23.
- [3] Bantan, R. A. R., Jamal, F., Chesneau, C. and Elgarhy, M. (2021). Theory and applications of the unit Gamma/Gompertz distribution. *Mathematics*, 9(1850), 1-22. <https://doi.org/10.3390/math9161850>
- [4] Casella, G. and Berger, R. L. (1990). *Statistical Inference*, Brooks/Cole Publishing Company: Bel Air, CA, USA.
- [5] Cordeiro, G. M. and dos Santos Brito, R. (2012). The beta power distribution. *Brazilian Journal of Probability and Statistics*, 26(1): 88-112.
- [6] Eliwa, S. M., Ahsan-ul-Haq, M., Al-Bossly, A. and El-Morshedy, M. (2022). A unit probabilistic model for proportion and asymmetric data: Properties and estimation Techniques with Application to Model Data from SC16 and P3 Algorithms. *Mathematical Problems in Engineering*, Article ID 9289721, <https://doi.org/10.1155/2022/9289721>
- [7] Galton, F. (1883). *Enquiries into Human Faculty and its Development*. Macmillan & Company, London
- [8] George, R. and Thobias, S. (2017). Marshall-Olkin Kumaraswamy distribution. *International Mathematical Forum*, 12(2): 47-69.
- [9] Ghitany, M., Al-Mutairi, D., Balakrishnan, N. and Al-Enezi, I. (2013). Power Lindley distribution and associated inference. *Computational Statistics and Data Analysis*, 64: 20-33.
- [10] Gilchrist, W. (1997). Modelling with quantile distribution functions, *Journal of Applied Statistics*, 24(1): 113-122.
- [11] Golshani, L. and Pasha, E. (2010). Renyi entropy rate for Gaussian processes. *Information Sciences*, 180: 1486-1491.
- [12] Gómez-Déniz, E., Sordo, M. A. and Calderín-Ojeda, E. (2014). The Log-Lindley distribution as an alternative to the beta regression model with applications in insurance. *Insurance: Mathematics and Economics*, 54(1): 49-57.

- [13] Gordon-Rodriguez, E., Loaiza-Ganem, G. and Cunningham, J. P. (2020). The continuous categorical: a novel simplex-valued exponential family. In 36th International Conference on Machine Learning, ICML 2020. International Machine Learning Society (IMLS).
- [14] Jamal, F., Chesneau, C., Aidi, K. and Ali, A. (2021). Theory and application of the power Ailamujia distribution, *Journal of Mathematical Modeling*, 9(3): 391-413.
- [15] Korkmaz, M. C., Altun, E., Chesneau, C. and Yousof, H. M. (2021). On the unit-Chen distribution with associated quantile regression and applications. *Mathematica Slovaca*, (to appear).
- [16] Korkmaz, M. and Chesneau, C. (2021). On the unit Burr-XII distribution with the quantile regression modeling and applications. *Computational and Applied Mathematics*, 40(1): 1-26.
- [17] Kumaraswamy, P. (1980). A generalized probability density function for doubly bounded random process. *Journal of Hydrology*, 46: 79-88.
- [18] Lindley, D. V. (1958). Fiducial distributions and Bayes theorem. *Journal of the Royal Statistical Society, Series B*, 20(1): 102-107.
- [19] Loaiza-Ganem, G. and Cunningham, J.P. (2019). The continuous bernoulli: fixing a pervasive error in variational autoencoders. In *Advances in Neural Information Processing Systems*, 13266-13276.
- [20] Mazucheli, J., Menezes, F. A. and Dey, S. (2019). Unit-Gompertz distribution with applications. *Statistica*, 79(1): 25-43.
- [21] Menezes, A. F. B., Mazucheli, J. and Dey, S. (2018). The unit-logistic distribution: different methods of estimation. *Pesquisa Operacional*, 38(3): 555-578.
- [22] Moors, J. J. (1988). A quantile alternative for kurtosis. *Statistician*, 37: 25-32.
- [23] Opone, F. C., Akata, I. U. and Osagiede, F. E. U. (2023). The Kumaraswamy unit-Gompertz distribution and its application to lifetime dataset. *Earthline Journal of Mathematical Sciences*, 11(1): 1-22.
- [24] Opone, F. C. and Ekhosuehi, N. (2017). A study on the moments and performance of the maximum likelihood estimates (mle) of the beta distribution. *Journal of the Mathematical Association of Nigeria (Mathematics Science Series)*, 44(2): 148-154.
- [25] Opone, F. C. and Iwerumor, B. N. (2021). A new Marshall-Olkin extended family of distributions with bounded support. *Gazi University Journal of Science*, 34(3): 899-914.
- [26] Opone, F. C. and Osemwenkhae, J. E. (2022). The transmuted Marshall-Olkin extended Topp-Leone distribution. *Earthline Journal of Mathematical Sciences*, 9(2): 179-199.
- [27] Quesenberry, C. and Hales, C. (1980). Concentration bands for uniformity plots. *Journal of Statistical Computation and Simulation*, 11(1): 41-53.
- [28] Rady, E. A., Hassaine, W. A. and Elhaddad, T. A. (2016). The power Lomax distribution with an application to bladder cancer data. *SpringerPlus*, 5, 1838.
- [29] Stock, J. H. and Watson, M. W. (2007). *Introduction to Econometrics*, 2nd ed., Addison Wesley: Boston, MA, USA. Available online: <https://rdrr.io/cran/AER/man/GrowthSW.html>
- [30] Wang, K. and Lee, M. (2020). Continuous Bernoulli distribution: simulator and test statistic. DOI: 10.13140/RG.2.2.28869.27365